



Production of the ZnO-folic acid nanoparticles and poly(vinyl alcohol) nanocomposites: investigation of morphology, wettability, thermal, and antibacterial properties

Shadpour Mallakpour¹ · Maryam Lormahdiabadi¹

Published online: 10 August 2020

© The Polymer Society, Taipei 2020

Abstract

The packaging system is one of the most challenging researches, in which antibacterial agents were embedded. In this research activity, we used folic acid (FA), as a biosafe and biodegradable substance for the surface modification of zinc oxide nanoparticles (ZnO NPs). Then, the ZnO-FA NPs as nanofillers were inserted in the poly(vinyl alcohol) (PVA) with different weight percentages (2, 5, and 8 wt%, relative to polymer weight). The synthesized substances were characterized using various analyses like Ultraviolet-Visible (UV-Vis) spectroscopy, water contact angle, field emission scanning electron microscopy, and thermogravimetric analysis. The image of transmission electron microscopy analysis displayed the excellent dispersal of the ZnO-FA NPs within the polymeric matrix. By increasing the percentage of the modified ZnO NPs into the PVA, the intensity of the absorption peaks in the UV-Vis spectra was raised, and the thermal stability of NC films got better compared to the pure polymer. PVA/ZnO-FA NC film 8 wt% showed better antibacterial activity than the pure PVA and had the best resistance against Gram-positive bacteria (*Staphylococcus aureus*).

Keywords Antibacterial activity. Optical property. Sonochemical approach. Folic acid. Poly(vinyl alcohol)

Introduction

Nowadays, one of the most important applications of the active packaging system is antibacterial packaging for food production. It is a system of packaging that can control the growth and inhibition of the activity of microorganisms, which can make food contamination. Some of the nanoparticles (NPs) have excellent antibacterial activity and can interact with the cell membrane of bacteria because of their high surface-of-volume ratio. Hence, NPs have been recognized as nanofillers for making nanocomposite (NC) films to enhance their packaging performance [1, 2].

Among all of the polymers, poly(vinyl alcohol) (PVA) is introduced as a semi-crystalline polymer that has specific characteristics such as high chemical resistance, the capability to form the film, the good mechanical strength, solubility in hot and cold water, and biodegradability. This polymer has been widely considered in a variety of fields including textile, industry, adhesive, fuel cells, and so on. PVA contains a large number of OH functional groups that produce hydrogen bonding and can interact well with organic and inorganic materials [3–5].

The variety of NPs and their usage have been dramatically increased in various fields due to their specific features. Such as TiO₂ that is considered in fabrication of wave-absorbing composites [6] or Fe₃O₄, which is attracted the attention of researchers because of its strong magnetic and low electrical conductivity properties [7]. Different NPs have been used for the reinforcement of PVA NC films such as TiO₂ [8], Ag [9], PbO [10], Fe₃O₄ [11], and so on. Among them, zinc oxide (ZnO) nanoscale has been considered for its superior features. These crystalline NPs in addition to being non-toxic, have the antibacterial trait and photocatalytic capability, and these bio-safe NPs have a large band gap and high excitation binding energy, which make them susceptible to use in the field of catalyst, solar cells, and optoelectronics [12, 13].

Electronic supplementary material The online version of this article (<https://doi.org/10.1007/s10965-020-02200-7>) contains supplementary material, which is available to authorized users.

✉ Shadpour Mallakpour
mallak@iut.ac.ir; mallak777@yahoo.com

¹ Organic Polymer Chemistry Research Laboratory, Department of Chemistry, Isfahan University of Technology, Isfahan 84156-83111, Islamic Republic of Iran

Fernandesa et al. [14] prepared PVA NC films with various percentages of ZnO NPs. Under inert atmosphere, they observed that the pure PVA films were thermally more stable than the PVA/ZnO NC films, and the existence of ZnO enhanced the crystallinity of the PVA NC films but could not improve the violence of the NC films. The solvent casting process was applied to prepare PVA and its NC films. At 20% mole of ZnO NPs, the crystallinity decreased owing to the variation in crystallite size and aggregation [15]. Ahangar et al. [16] created PVA-ZnO NC films by casting solution procedure. They observed that the increment of ZnO NPs into the PVA biopolymer reduced the transparency of the NC films and upturned the antibacterial activities, but NPs tended to accumulate at a point in the NC films.

For better dispersion of NPs and preventing their aggregation, researchers have been tried to modify the surface of NPs with other molecules. Tang et al. [17] used the sonochemistry method to graft ZnO NPs with poly(methacrylic acid) (PMAA). The thermogravimetric analysis (TGA) showed that the modified ZnO NPs with PMMA reduced the agglomeration of ZnO NPs. Chakradhar et al. [18] described an eco-friendly approach to modify ZnO NPs with stearic acid (ZnO@SA). They found that the surface modification developed a superhydrophobic property of the NPs' surface; thus, this feature can be used to build micro/nanoscale devices. Other materials, which can be used for the modification of ZnO NPs are bovine serum albumin [19], diacids based on amino acid [20], vitamin B1 [21], citric acid [22], β -cyclodextrin [23], etc.

The vitamin B family contains folic acid (FA) (also known as vitamin B9), is an orange-yellow crystalline powder and an artificial form of folate. FA is slightly soluble in water and is susceptible to light and heat. This vitamin is easily found in many foods, such as broccoli, orange, peas, and so on. Functional groups in this tasteless and odorless substance are imino, amino, hydroxyl, imide, carboxyl, and tertiary amine, which can easily form intermolecular hydrogen bonding. [24, 25]

A few studies have shown the modification of ZnO NPs with FA. Muhammad et al. and also Ma et al. [26, 27] used amine groups to synthesize the ZnO-NH₂ quantum dots (QDs). Toxic solvents such as 1-ethyl-3-(3-dimethylaminopropyl) carbodiimide and dimethyl sulfoxide were used to activate the carboxylic (COOH) groups of FA. Finally, the achieved products were ZnO-FA QDs that were used for targeted cancer cell imaging.

In this paper, we used the sonochemical method as a green and safe technique to modify NPs and prepare PVA NCs. The sonication method leads up better dispersion of ZnO-FA NPs in the polymeric matrix. By this method, it does not require much temperature to carry out effective attractions, also these attractions even have the potential to occur at ambient temperatures by utilizing the energy of ultrasonic waves. The mode of operation is such that vibrations occur through the ultrasonic wave and then propagation into the initial fluid through

which bubbles form in the fluid. The bubbles are created, grown, and reached a critical size; inside the bubbles of critical size, localized regions with high pressure and high temperature (about 5000 K), with stability within the nanosecond. Eventually, an explosion of a series of bubbles produces a shock wave. The energy generated by this shock wave is used to break down covalent bonds, homogenize, perform specific chemical reactions, especially the synthesis of NPs, organic materials, and so forth. [28, 29]

In this study, firstly we endeavored to apply the ultrasound technique to develop the attributes of PVA as a polymeric matrix with ZnO-FA NPs. In the second step, the characterization and properties of PVA/ZnO-FA NC films were evaluated. At last, the antibacterial activity of the pure PVA and PVA/ZnO-FA NC film 8 wt% were assessed against *Staphylococcus aureus* (*S. aureus*, ATCC 12600) and *Escherichia coli* (*E. coli*, ATCC 9637) bacteria using the liquid medium microdilution method.

Experimental

Practical materials

The white powder of ZnO NPs (average particle size = 25–30 nm) with a specific surface area $> 60 \text{ m}^2 \cdot \text{g}^{-1}$ was acquired from Neutrino Company (Tehran, I. R. Iran). FA was procured from Acros Organics Company (Belgium). PVA with $M_w = 145,000 \text{ g} \cdot \text{mol}^{-1}$ and *N,N'*-Carbonyldiimidazole (CDI) were acquired from Merck Chemical Company (Darmstadt, Germany). Deionized water (DIW) was received from the Kowsar Company (Isfahan, I.R. Iran).

Characterization methods and instruments

For preparing the modified NPs, the TOPSONICS ultrasonic liquid processor (Tehran, I. R. Iran) with the power of 100 W and frequency wave of 20 kHz was used. The NC films were rigged with ultrasound output waves from the UP-100 series of TOPSONICS ultrasonic liquid processor (Tehran, I. R. Iran) by the power of 400 W and frequency 20 kHz. Both devices were equipped with a probe. All the FT-IR spectra were obtained, using a Jasco-680 spectrometer (Tokyo, Japan), which has a resolution of 4 cm^{-1} and reports the wave-number in the range of $4000\text{--}400 \text{ cm}^{-1}$. For powder samples, the potassium bromide (KBr) pellets were provided, which the ratio of sample to KBr was 30:100. To study the crystallinity structures of ZnO-FA NPs and PVA/ZnO-FA NC films, X-ray diffraction (XRD) patterns were gathered by the Philips X'Pert MPD diffractometer (Germany) with $2\theta = 10\text{--}80^\circ$ and the rate of $0.05^\circ/\text{min}$ using Cu K α source and a beam of $\lambda = 1.540 \text{ nm}$. The UV-Vis spectra of the specimens were obtained using Jasco V-570 spectrophotometer (Tokyo, Japan) in

the range of 25 to 800 nm. To peruse the thermal behavior of the samples, they first were dried in a vacuum pump at the temperature range of 50–60 °C, and then the corresponding test was carried out at 25–800 °C using a STA6000 Waltman (USA) apparatus and the speed of applied heat was 20 °C.min⁻¹ under an argon atmosphere. The micrographs of field emission scanning electron microscopy (FE-SEM) exhibited the dispersal of ZnO-FA NPs on the surface of the PVA matrix and their morphology was collected by HITACHI (S-4160). By using Philips (CM 120, Netherlands) microscope with a voltage 100 kV, the images of transmission electron microscopy (TEM) were achieved. To obtain TEM images, modified NPs and NC films were dispersed in DIW by ultrasonic irradiation, next a drop of supernatant was placed on copper grid and dried. Then the images were taken. The size of NPs was measured by applying the Digimizer 4.6.1.0 software, and the results were calculated and examined via the SPSS Statistics 17.0 software. The specimens were cut into size 40 mm × 20 mm and then the test of tensile was done by the related device [Testometric Universal Testing Machine M350/500 (UK)]. The speed of this test was adjusted at 20 mm.min⁻¹. Wetting characteristics of the prepared NC films were recorded using digital microscopy camera U-VISION MV500 that was manufactured in China. For the elemental analysis of the specimens, the energy dispersive X-ray (EDX) spectroscopy was accomplished by way of Tescan Mira II spectrometer (Czech Republic). Precise measurement of specific surface area and porosity was performed with a BELSORP MINI II (Japan).

Production of coating ZnO NPs with FA

In the first step, 20 mg (453×10^{-7} mol) of FA was dispersed into 8 mL of DIW and agitated. After 2 h, by adding 7 mg (413×10^{-7} mol) of CDI and stirring for 5 h, a bright yellow solution was seen. This process was performed to activate FA. At the second step, 100 mg of ZnO NPs were added up to 8 mL of DIW and stirred for 2 h, then were exposed to ultrasonic waves for 5 min and power of 60 W (7 s on and 3 s off) for the dispersion of NPs. After that, the suspension of NPs was added to the solution of FA. After stirring overnight, the suspension was exposed to ultrasonic irradiation with a power of 70 W and a duration of 30 min. This suspension was washed with distilled water and centrifuged for 8 min for four times to remove impurities. Then the resulting sediment was dried at ambient temperature (Scheme 1).

Assembling of the PVA/ZnO-FA NC films

To prepare the PVA stock solution, 300 mg of PVA powder was dissolved in the 50 mL of DIW at 95 °C for 2 h. To fabricate the PVA NC films, three distinct quantities of the dried ZnO-FA NP powders were used. In this way, the

amounts of 2, 5, and 8 wt% of the modified ZnO NPs (respect to the PVA weight) separately were added to the PVA solution and agitated magnetically for 2 h with high rapidity. After that, to obtain a perfect homogeneity, this suspension was ultrasonicated for 30 min at a power of 70 W. Immediately after disclosure under ultrasound, the mixture was poured into two clean and dry plastic Petri dishes into an equal volume and then were placed under the clean hood to vaporize the solvent, and the NC films were created.

For the preparation of the NC films with better transparency, the dried NC films were crushed and added to the 50 mL of DIW and then were heated at 95 °C for 30 min at the same time. After that, ultrasonication was applied on the suspension for 15 min at a power of 70 W. At the following step, the blend in the Petri dishes turned into NC films after 2 days (Scheme 1).

Antibacterial assays

The antibacterial activity of the pure PVA and PVA/ZnO-FA NC film 8 wt% against *S. aureus* and *E. coli* was assessed by using liquid medium microdilution methods like the quantitative analysis. The standardized bacteria solution was prepared by fresh inoculation colonies of *E. coli* and *S. aureus* strains into 5 mL nutrient broth medium (QUELAB, England) and incubation at 37 °C overnight. After that, the suspensions were diluted to approach an absorbance value of 0.1–0.2 ($\lambda_{\max} = 625$ nm). Afterward, the prepared samples were made up to 10 mg and appended on to the fabricated bacterial suspensions and incubated with gentle agitation at 37 °C and the speed of 80 rpm.min⁻¹ on a shaker platform (Eppendorf Thermo-mixer, Germany) for 24 and 48 h. The UV-Vis spectrophotometer was applied to obtain the absorbance value of all samples at the determined time. The following equation was used to calculate the bacterial inhibition percentage:

$$\text{Bacterial inhibition (\%)} = [(I_c - I_s)/I_c] \times 100 \quad (1)$$

I_c : the absorption extent of the control of bacteria suspension.

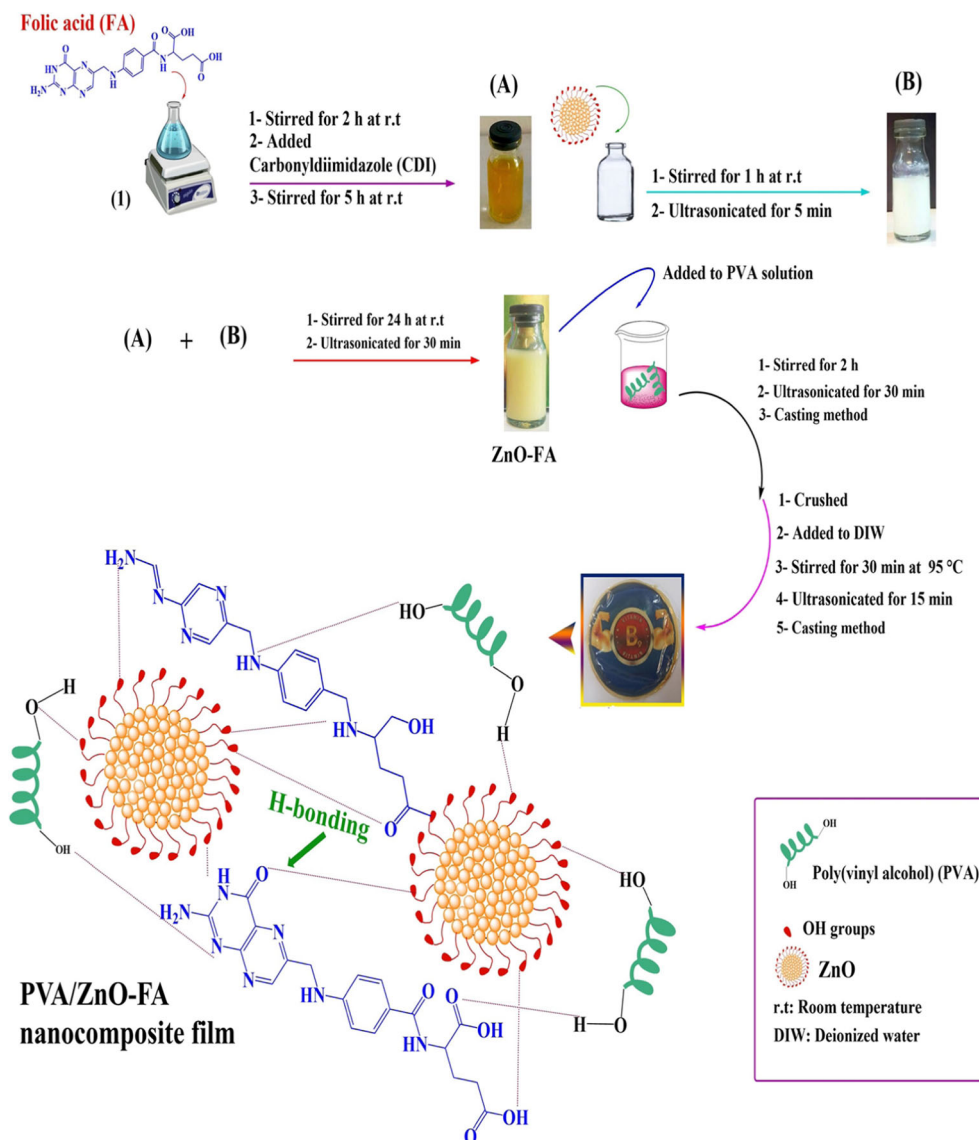
I_s : the absorption extent of the bacteria suspension included the different samples [30].

Results and discussion

Pure ZnO NPs have low stability in water and easily accumulate; the reason for this phenomenon is the presence of hydroxyl groups on their surface, which have relatively high surface energy [31]. Three methods have been developed to improve the stability of NPs, such as (i). ball milling (ii) mechanical fluid shearing, and (iii). ultrasonic agitation [32].

The ultrasonic method and the modifier agent were used in this research to improve the dispersion of ZnO NPs. FA as a surface-modifying agent with carboxylic acid and amine

Scheme 1 A schematic illustration of ZnO-FA NPs and PVA/ZnO-FA NC films



functional groups, can establish the hydrogen bonds and the electrostatic interactions with the hydroxyl groups of the NPs and lead to breaking the agglomerates.

Figure 1(a) shows the stability of ZnO-FA NPs in DIW. The ZnO-FA NPs' suspension was stable for more than 10 days, but for the pure ZnO NPs under as same conditions as the modified ZnO, as soon as the container placed, sedimentations started, and complete phase separation was observed after 3 h, which shows the instability of the pure ZnO NPs [Fig. 1(b)]. This increment in the stability time can be attributed to the positive and undeniable impact of FA as a factor for surface modification.

Excellent dispersion stability of ZnO-FA NPs in the PVA solution after 30 min sonication effect can be observed in Fig. S1. While, if only magnetic stirrer was used, unstable dispersion and fast precipitation of the particles in the container would have been observed. Hence, the significant efficacy

of ultrasonic irradiation well is realized for stabilizing a polymer solution containing ZnO-FA NPs.

By increasing the concentration of ZnO-FA NPs in the polymeric matrix, the transparency of the NC films negligibly diminished, and their color turned to more yellowish (Fig. 2). Figure 3 shows the flexibility and non-brittle characteristics for PVA/ZnO NC film 5 wt%.

Investigation of the FT-IR spectra

Figure 4(a) indicates the spectrum of the pure FA, which the existence of two absorption bands in 3543 and 3414 cm^{-1} represent the stretching frequencies of the O–H in the acidic functional group and N–H bond, respectively. The stretching vibrations of the C–H and C=O bonds are appeared at 2925 and 1694 cm^{-1} , respectively, and the absorption band in 1605 cm^{-1} is associated with the N–H bending vibration.



Fig. 1 Dispersion stability of ZnO-FA NPs in DIW (a) and the pure ZnO NPs (b)

The absorption bands of the phenyl ring and pyridine in the FA structure are illustrated in 1697 and 1483 cm^{-1} , respectively [33, 34]. The pure ZnO NPs demonstrate the unique absorption band within the range of $590\text{--}400\text{ cm}^{-1}$. Also, due to the absorption of water molecules on the surface of the NPs, the characteristics of hydroxyl groups are shown in 3434 and 1638 cm^{-1} , which are belonged to the O-H stretching and bending vibrations, respectively [Fig. 4(b)] [35]. For the ZnO-FA NPs, a broad band is observed in 3366 cm^{-1} , that ascribed to the hydroxyl groups. The absorption bands in 2922 and 2852 cm^{-1} are allocated to the asymmetric and symmetric aliphatic C-H stretch vibrations of --CH_2 , respectively, which proved the presence of FA in the ZnO NPs structures. Owing to the hydrogen bonding between the ZnO NPs and the modifier agent, the band of the carbonyl group is detected in 1607 cm^{-1} , and the certain absorption band in 438 cm^{-1} is an evidence of the existence of ZnO NPs. Due to the formation of carboxylate salt, the symmetric and asymmetric stretching vibrations are associated with it appeared at 1510 and 1449 cm^{-1} [Fig. 4(c)] [36, 37].

In Fig. 5, the FT-IR spectra of the pure PVA and its fabricated PVA/ZnO-FA NC films are shown. The main characteristic bands of the pure polymer are observed at 3436 , 2940 , 1653 , and 840 cm^{-1} , which are arranged in sequence the stretching vibrations of OH, the asymmetric stretching CH_2 , the C=O stretching, the C-H bending and the C-C stretching vibrations. The differences between the pure PVA and the

Fig. 2 Visual transparency of the pure PVA (a) and PVA/ZnO-FA NC films of 2 wt% (b), 5 wt% (c), and 8 wt% (d)

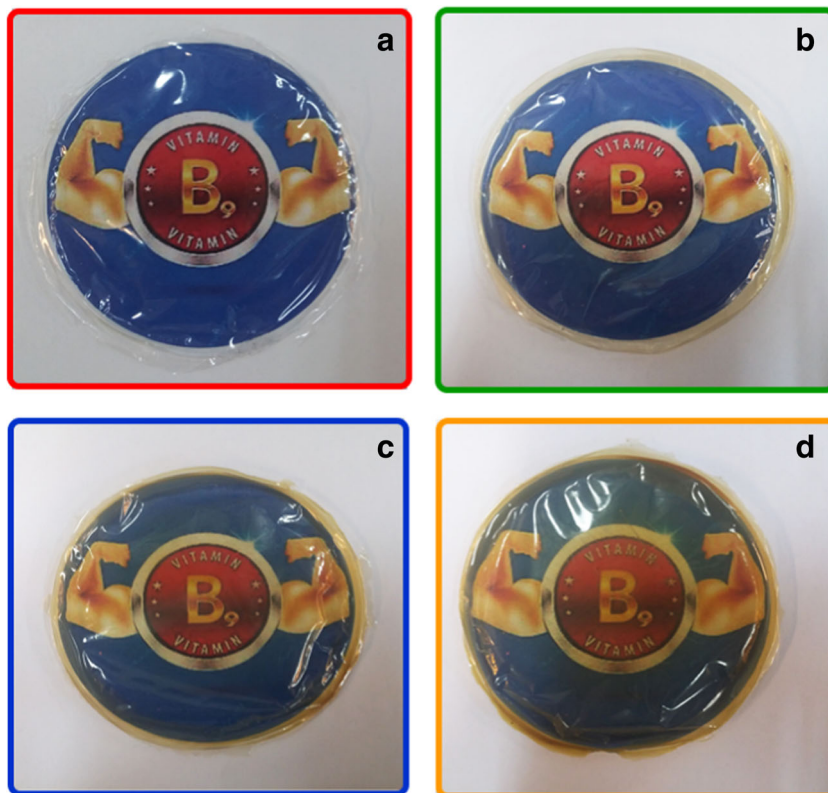




Fig. 3 Flexibility image of PVA/ZnO-FA NC film 5 wt%

fabricated PVA/ZnO-FA NC films are the existence of the absorption band in 424 cm^{-1} , because of the stretching vibration of Zn–O and appearance of a low-intensity band in 1607 cm^{-1} , that may be due to the existence of C=O groups in the structure of FA [38].

Examination of the XRD diagrams

Figure 6 depicts the XRD diagrams of the pure ZnO NPs, pure FA, and modified ZnO NPs. As seen in Fig. 6(a), reflection of (100), (002), (101), (102), (110), (103), (200), (112), and (201) revealed the hexagonal wurtzite form of the ZnO NPs [39]. The XRD diagram of the FA shows the crystallinity form for it [Fig. 6(b)]. To study the trace of FA on the crystalline structure of the ZnO NPs, the XRD diagram of the ZnO NPs was studied before and after the modification process, and there is no variation in the crystalline form of ZnO NPs after surface modification. A peak broadening was observed in the pattern of modified NPs, which is an indication of the effect of FA on the broadening of peaks and reducing the crystallinity of ZnO NPs [Fig. 6(c)].

The XRD diagram of the pure PVA indicates two regions, amorphous and crystalline phases, which are explanatory of

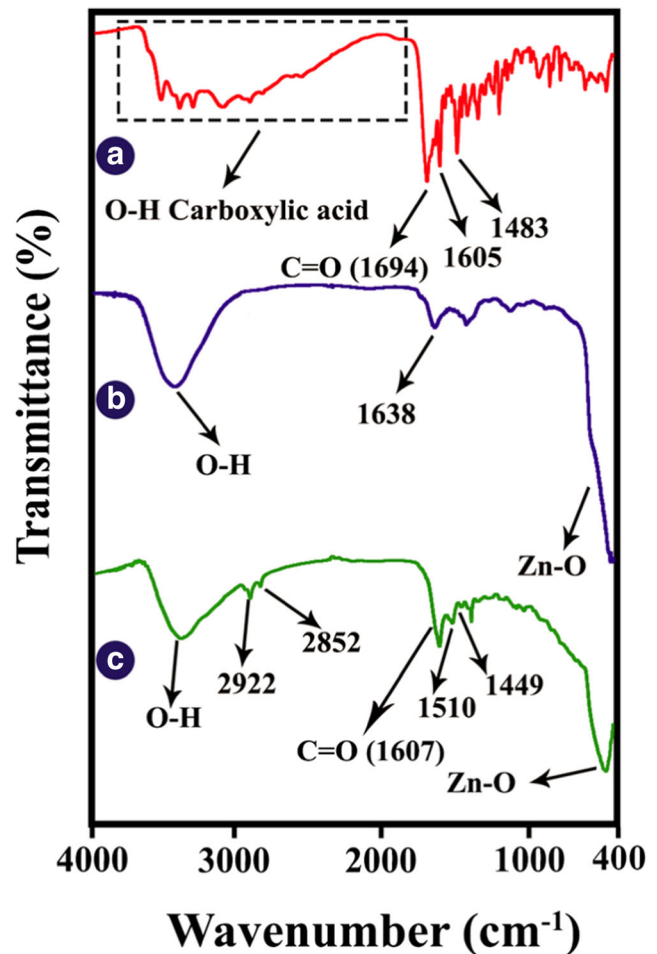


Fig. 4 FT-IR analysis of the pure FA (a), pure ZnO NPs (b), and ZnO-FA NPs (c)

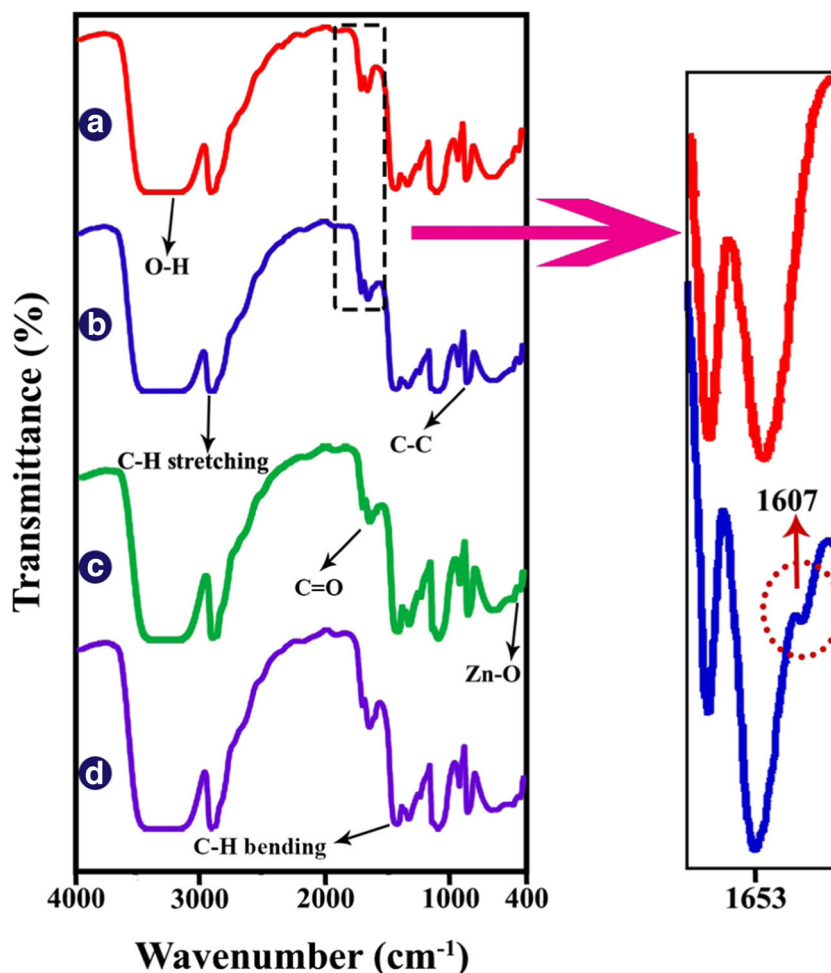
the semi-crystalline form that is associated with the hydrogen bonding in the polymer chain [Fig. S2(a)] [40]. In XRD diagrams of PVA/ZnO-FA NC films of 2, 5, and 8 wt%, new peaks with the 2θ values at 32, 34 and 36 are appeared. The intensity of these peaks increases by an increment of ZnO-FA NPs in NC films [Fig. S2(b-d)].

FE-SEM explorations

By moving a set of electron beams on the surface of the specimen and its bombarding, some photons and electrons remove from the specimen and release to the detector in which are transformed into a signal and finally a wide variety of information from the sample surface is provided [41].

By examination of the surface morphology of the ZnO-FA NPs by the FE-SEM, micrographs at various magnifications indicate a uniform spherical form for the NPs (Fig. 7). Regarding the FE-SEM micrograph for the pure PVA, a smooth surface is observed [Fig. 8(a)]. In literature studies, it was designated that ZnO NPs aggregated in the polymer matrix, but the bright and halo points in FE-SEM micrographs

Fig. 5 FT-IR analysis of the pure PVA (a), and PVA/ZnO-FA NC films of 2 wt% (b), 5 wt% (c), and 8 wt% (d)



clarify the existence of ZnO-FA NPs in the polymer, and it well illustrated the progressive effects of ultrasonic waves and FA as a modifier in order to disperse NPs in the PVA [Fig. 8(b)] [16, 42].

TEM studies

Using TEM, the structural and morphological aspects of the ZnO-FA NPs and PVA/ZnO-FA NC films were inspected, and the particle size of the ZnO-FA was estimated in the absence and the presence of a polymeric matrix using the corresponding histograms.

As can be observed from Fig. 9, NPs have a spherical structural morphology. In Fig. 9(c) at a magnification of 20 nm, a core-shell morphology is seen around the spherical NPs, which confirms the presence of the FA on the surface of the ZnO NPs. The average particle size for the pure ZnO NPs was reported between 20 and 30 nm, while for the modified ZnO NPs, the size has been increased to about 44 nm. This view submitted that NPs were well-functionalized with FA.

For TEM analysis, PVA/ZnO-FA NC film 5 wt% was selected because of its better dispersion. The TEM images of

this NC film in different magnifications present the good and uniform distribution of the ZnO-FA NPs in the PVA. Also, the size of the ZnO-FA NPs reduced with insertion in the PVA. It implied the establishment of H-bonding between OH groups from the backbone of PVA with functional groups in ZnO NPs and FA (Fig. 10). All the evidence points out to the undeniable power of ultrasound radiations to fracture the NPs accumulation and make them better and more homogeneous in the pure PVA, which cannot be achieved with the conventional methods.

UV-visible absorption spectroscopy

In order to investigate the optical features of NPs, and the PVA/ZnO-FA NC films, their UV-Vis spectra of them are studied (Figs. S3 and S4). The pure ZnO NPs have a specific peak which is seen at 365 nm [43]. The absorption peaks for the pure FA reveal in 280 nm (π - π^* transition) and 360 nm (n - π^* transition) [44]. Increasing the absorption was observed for the modified ZnO-FA NPs, which is owing to the presence of FA on the surface of the NPs.

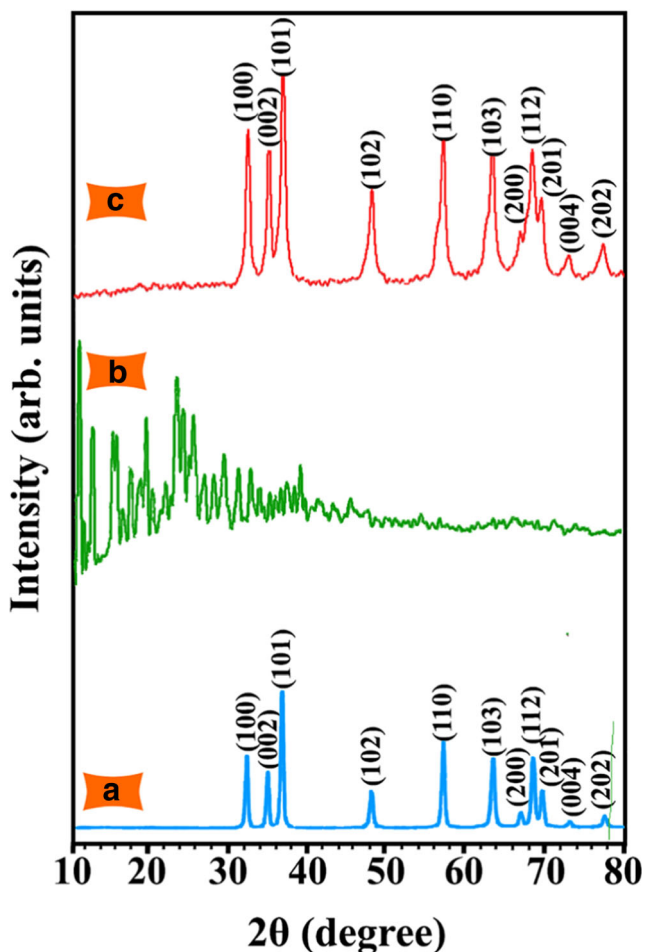


Fig. 6 The XRD diagrams of the pure ZnO NPs (a), pure FA (b), and ZnO-FA NPs (c)

The absorption peak at 260 nm is related to the $n\text{-}\pi^*$ electron transition for the pure PVA, while in the NC films of PVA/ZnO-FA, the absorption bands of NPs and FA can be detected. The absorption intensity increments with an increase in the percentages of ZnO-FA NPs but no shift for the wavelength is seen (Fig. S4).

EDX inspections

The attendance of elements such as carbon (C), oxygen (O), and nitrogen (N) are recognized, which proposes that the ZnO NPs were modified by FA (Table 1 and Fig. S5). The presence of sulfur (S) with a minimal amount (2.15 wt%) in this outcome may be related to the use of sulfur compounds in the synthesis of FA [45].

The results for PVA/ZnO-FA NC film is accessible (Table 2 and Fig. S6). An increase in the weight percentage of C from 18.28 wt% in the ZnO-FA NPs to 54.69 wt% in the NC film can well be pointed to the presence of PVA.

Mechanical performance

In order to examine the mechanical properties of NC films, a rectangular piece of the sample was sealed between the two metal jaws, while the lower jaw was constant, the top moved upward at a constant velocity ($20 \text{ mm}\cdot\text{min}^{-1}$) until the sample tears [46]. The outcomes of this test are summarized in Fig. 11 and Table 3. Mechanical performance is affected by factors such as the amount, size, morphology of NPs, quality, functionality, and distribution of them on the surface of the polymeric matrix and interactions between the polymer and modified ZnO NPs. Moreover, The agglomeration of NPs, trapping gas in the process, which could damage the structure of NPs, may contribute to the degradation of mechanical properties [47]. The amount of the Elastic modulus (E -modulus) for NC films are generally lower than the pure polymer when the concentration of ZnO-FA NPs increased; this may be due to the large amounts of NPs in the polymer matrix, which may change the general condition and effects on the structure of the polymer, and its interaction with the polymer disrupting the interaction between the polymer chains. Also, NPs is more stiffness than a polymer and easily could nest within the space of polymer chains and as limitation factors exert constraint into the molecular mobility of the polymer chains. Therefore, the rough nature of ZnO NPs can disable NC films

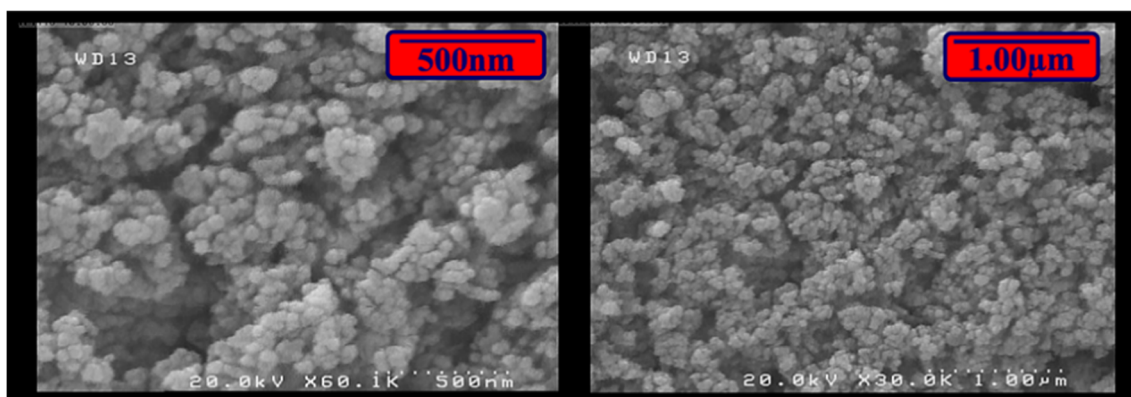


Fig. 7 The FE-SEM micrographs of the ZnO-FA NPs at several magnifications

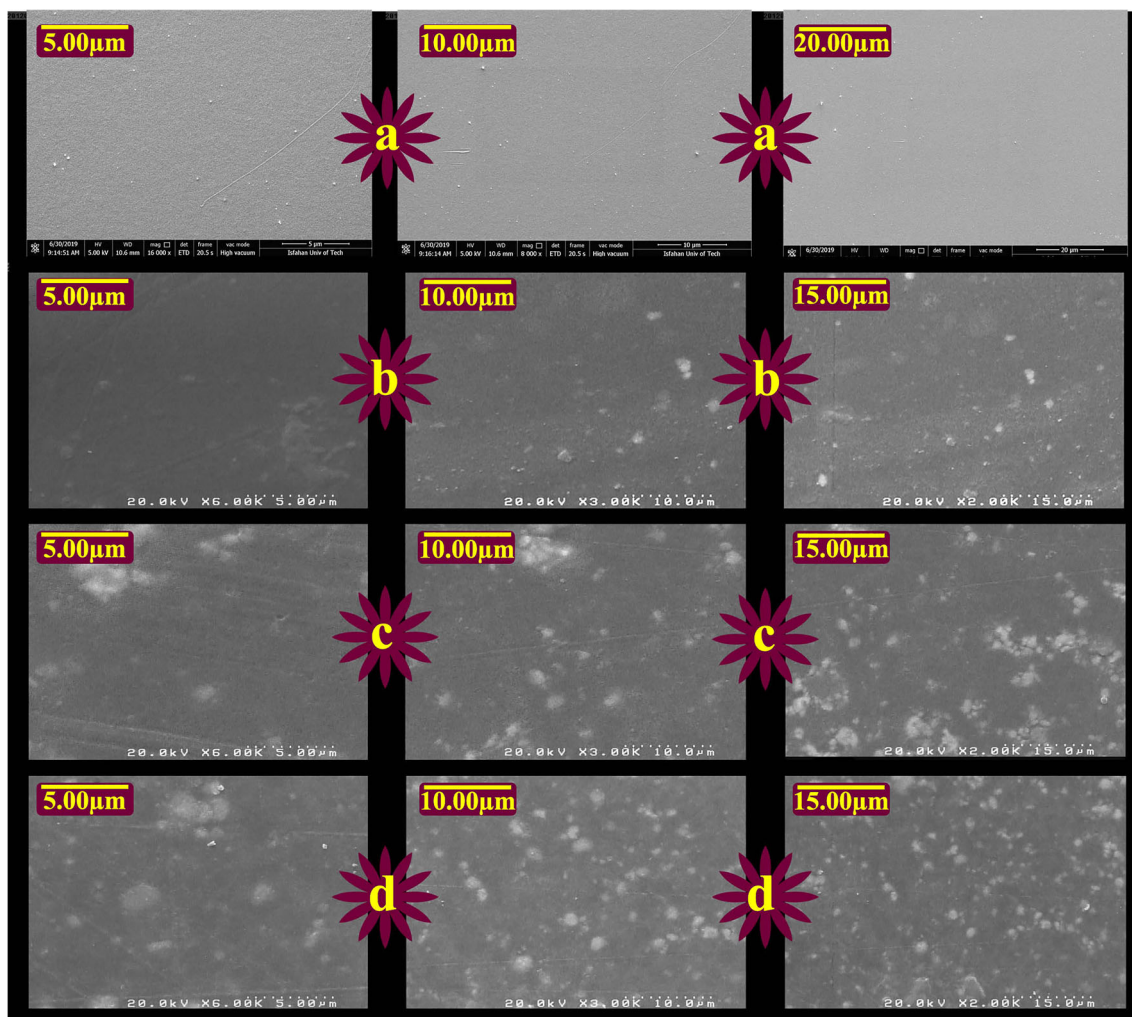


Fig. 8 The FE-SEM micrographs of the pure PVA (a), and PVA/ZnO-FA NC films of 2 wt% (b), 5 wt% (c), and 8 wt% (d)

to be enough flexible. Consequently, by adding smaller amounts of nanoparticles in this case, mechanical strength might be improved [16].

BET surface area analysis

This analysis is used to study the specific surface area of the NPs by using the adsorption-desorption (ADS-DES) process of nitrogen gas (N_2) at 77 K. [48]. The data about the surface area of the pure ZnO NPs and the ZnO-FA NPs has dropped from 41 down to 21 $m^2.g^{-1}$, which presented successful modification of the NPs' surface. Actually, FA has covered pores of the sample and decreased the surface area. Figure 12 displays N_2 ADS-DES isotherm curves for ZnO-FA, which the observed isotherm is compatible with type IV isotherm and

the type of hysteresis loop is H3; these commentaries confirm mesoporous structure [49–51].

Wettability

The contact angle (CA) test is used to check the hydrophilic and hydrophobic properties of the samples. (i) The measurements of a liquid droplet in an air atmosphere, (ii) the measurements of a liquid droplet under liquid conditions, and (iii) the measurements of the air bubble under liquid conditions are three categories that are used to quantify the CA. When the amount of CA is below 90°, referred to as the hydrophilic trait, but for the hydrophobic feature, the CA value is upper than 90°. For this reason, with a syringe containing food color, three droplets were placed in different regions of NC films and after a short time, a shot took from the drop on the

Fig. 9 The TEM images of the ZnO-FA NPs at various magnifications (a-c)

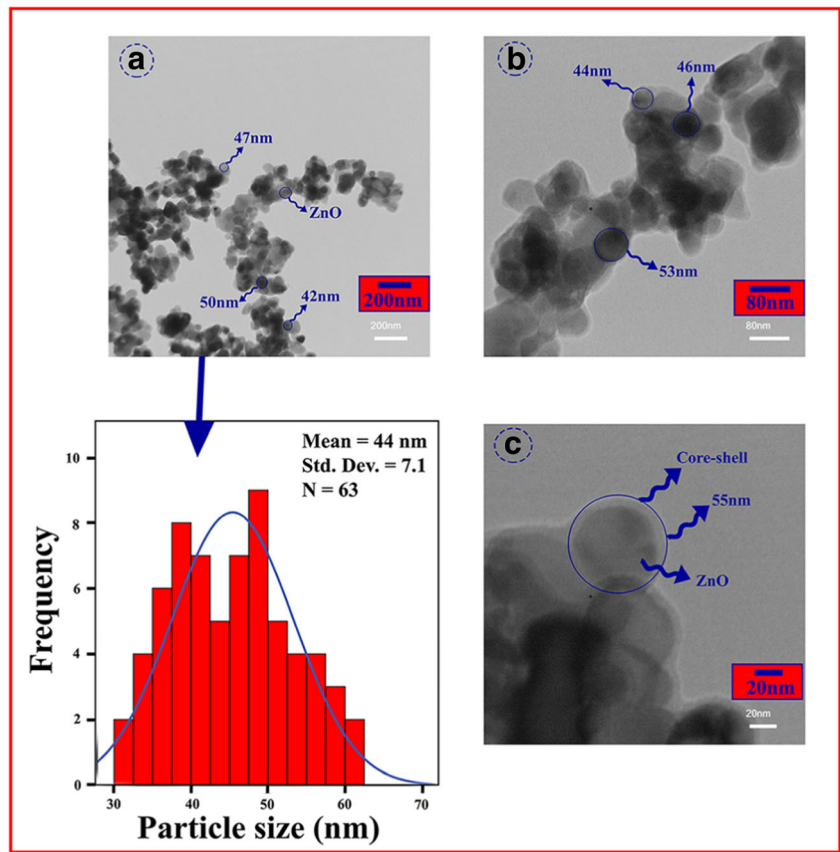


Fig. 10 TEM images of PVA/ZnO-FA NC film 5 wt% at various magnifications (a-c)

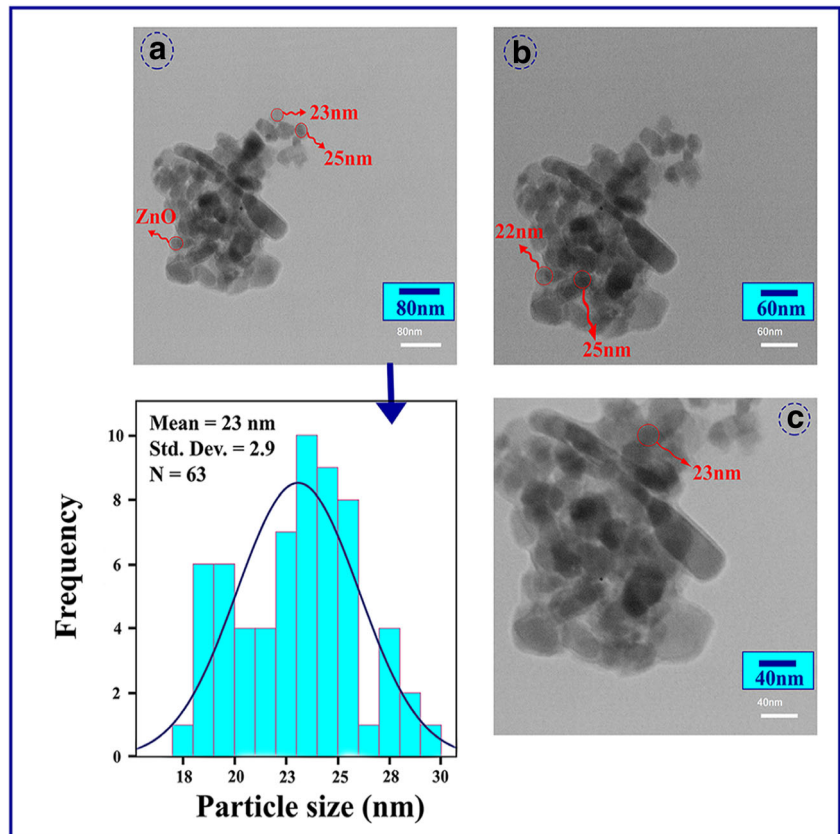


Table 1 Kinds of elements and their percentages in ZnO-FA NPs

Elements	Line	wt%	Intensity
C	Kα	18.28	8.2
N	Kα	12.04	3.6
O	Kα	48.11	50.3
S	Kα	2.15	21.8
Zn	Kα	19.41	39.8

polymer surface, and this analysis repeated three times. The CA images for the obtained NC films as well as the average amounts of CA and standard deviations are listed in Table 4. To compare these data, the least significant difference (LSD) and One-Way analysis of variance (ANOVA) tests were operated. According to CA images and the outcomes in Table 4, NPs-containing NC films have a hydrophilic property. This feature is reduced by increasing the amount of the ZnO-FA NPs in the polymer, but for the NC film with 8 wt% of ZnO-FA NPs, the angle between surface and droplet decreased. The reason for this phenomenon may be due to the agglomeration of the NPs in the polymer at this percentage. The value of ρ reported 0, which means values reflected statistically significant [52, 53].

Thermal properties

In the TGA curve of pure ZnO NPs, the minor reduction is perceived, which is associated with the elimination of water that physically absorbed on the surface of NPs, but there is no significant reduction in weight in the temperature range [54]. For ZnO-FA NPs, the thermogram presents a mass loss in three main stages. The first stage is related to the dehydration of the sample. The decomposition of FA becomes evident in the second step in the range of 200–650 °C. In the third step, the organic samples are pyrolyzed and produced black carbon, thus, the observed mass loss in the range of 700–800 °C is relevant to the formation of carbon black and ash. (Fig. 13) [55] According to the TGA curves of the pure ZnO NPs and ZnO-FA NPs, approximately 13% of FA was grafted on to the surface of ZnO NPs.

In Fig. 14 the thermal stability behavior of the pure polymer and fabricated PVA/ZnO-FA NC films are reviewed. In all curves, three principal mass losses are seen. In the

Table 2 The results of the EDX outcomes of PVA/ZnO-FA NC film 5 wt%

Elements	Line	wt%	Intensity
C	Kα	54.69	160.0
N	Kα	13.89	5.4
O	Kα	30.79	47.9
Zn	Kα	0.64	0.8

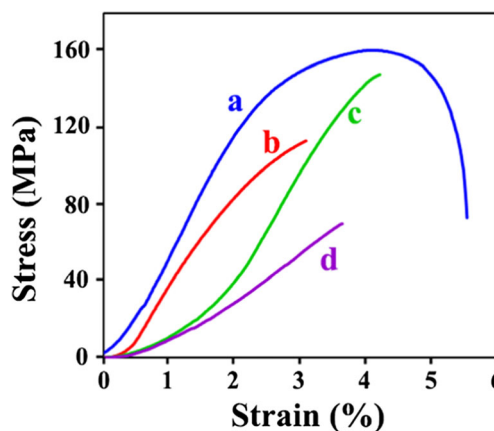


Fig. 11 The Stress-Strain curves of the pure PVA (a), and PVA/ZnO-FA NC films of 2 wt% (b), 5 wt% (c), and 8 wt% (d)

temperature range of 50–170 °C, the observed mass loss is ascribed to the vaporization of the remaining solvent and the weakly physical and strong chemical bound water. A massive drop in the area of 230–370 °C is related to the decay of the hydroxyl groups as a side chain in the polymer chain, and the third stage of mass occurred in the area of 370–480 °C showed carbonation which means the fracture of the C–C backbone of the PVA [56, 57].

Table 5 displays temperature information when the mass loss is 10% ($T_{10\%}$) and 50% ($T_{50\%}$) in the NC films, and also the percentage of residual weight at 800 °C [char yield (CY)]. It shows that the thermal resistance of the NC films measures up to the pure PVA has significantly increased, according to the information of Table 5. Concerning the data of DTG curves (Fig. S7), T_{max} (the temperature where a sudden mass loss of the specimen happened) can be achieved. The values of T_{max} are raised to 16 °C, 40 °C, and 50 °C for PVA/ZnO-FA NC films 2, 5, and 8 wt% compared to the pure PVA, respectively. There is also an increase in the CY values for NC films which have ZnO-FA NPs. These results inferred strong interactions between PVA and ZnO-FA NPs, which caused the movement of polymer chains near the surface to be decreased [58].

Antibacterial activity

The antibacterial property of the PVA/ZnO-FA NC film 8 wt% was assessed against *E. coli* and *S. aureus* as Gram-negative and Gram-positive bacteria for 24 and 48 h, respectively. As shown in Fig. 15, pure PVA has no antibacterial property and cannot inhibit bacterial growth, but the addition of ZnO-FA NPs to the PVA matrix can improve the antibacterial property, and over time, bacterial growth is stopped further. The bacterial inhibition by PVA/ZnO-FA NC film 8 wt% is because of the presence of metal oxides such as ZnO NPs which carry the positive charges, whereas the microorganisms move the negative charges. This difference in the type of charges leads to electrostatic interactions between

Table 3 The mechanical characterization of the pure PVA and fabricated PVA/ZnO-FA NC films





Samples	<i>E</i> -modulus (MPa)	Elongation (mm)	Stress (MPa)	Strain (%)
Pure PVA	5052	1.7	160	4.2
PVA/ZnO-FA NC film 2 wt%	4273	1.2	113	3.1
PVA/ZnO-FA NC film 5 wt%	2319	1.7	148	4.2
PVA/ZnO-FA NC film 8 wt%	1828	1.5	70	3.6

ZnO NPs and organisms, which causes oxidation and finally death of organisms [59]. The percentage of bacterial inhibition is tabulated in Tables 6 and 7.

The results show the higher activity of PVA/ZnO-FA NC film 8 wt% against *S. aureus* in contrast with *E. coli*. The

discrepancy in the cell structure, physiology, metabolism, and the degree of contact of organisms with ZnO NPs may be the reasons for the difference in the resistance against the Gram-negative and the Gram-positive bacteria. As an example, *S. aureus* has more carboxyl and amine groups on its cell

Table 4 The results and images of CA for pure PVA and prepared NC films [mean (standard deviation)].

Sample	CA (°)	Images
Pure PVA	77 (0.94)	
PVA/ZnO-FA NC film 2 wt%	81 (1.29)	
PVA/ZnO-FA NC film 5 wt%	87 (0.92)	
PVA/ZnO-FA NC film 8 wt%	76 (0.82)	

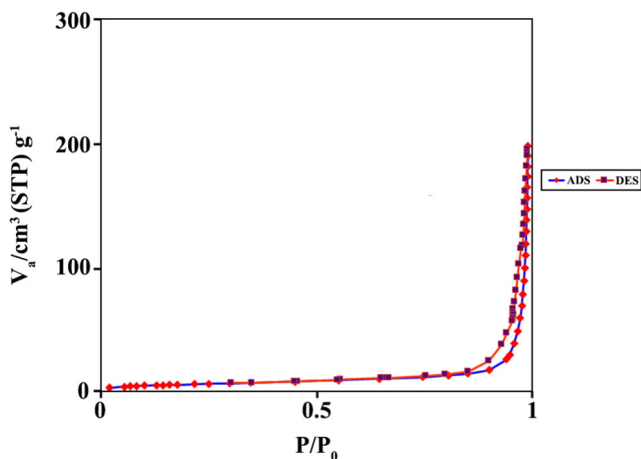


Fig. 12 N_2 ADS-DES isotherm curve of ZnO-FA NPs

surface, so more dependencies exist between ZnO NPs and these groups [60, 61].

Conclusions

In the present study, the first effort was made to amend the properties of PVA by placing ZnO NPs in the polymeric matrix. While for better dispersion, FA was applied as a modifying agent. The most significant tool which was utilized in this investigation was an ultrasonic device. The yielded ultrasonic waves not only reduce the procedure time but also allow to do reactions that are not possible with conventional approaches. In the dispersion stability test, FA had an impressive role in stabilizing ZnO NPs. Also, sonication waves had remarkably influence on the good distribution of the modified ZnO NPs in the solution of the polymeric matrix. According to the previous results, the obtained data from FT-IR and EDX analyses are easily verified that, as expected, the ZnO NPs with FA have been modified. As well as the shifts of band locations in the FT-IR spectrum can be explained hydrogen and electrostatic interactions. The thermal properties were checked, and the obtained outcomes presented that PVA/ZnO-FA NC films 5, and 8 wt% have better thermal stability because there

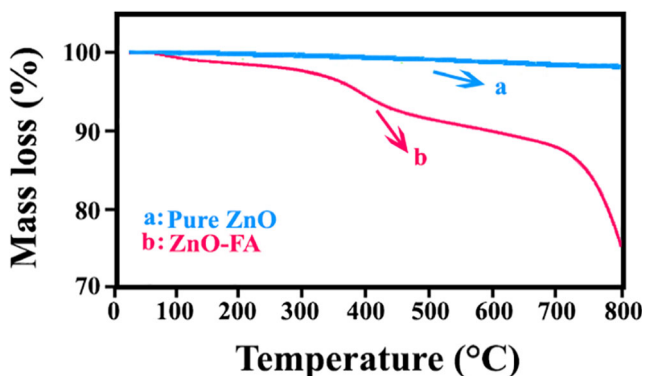


Fig. 13 The TGA curves of the pure ZnO NPs (a) and ZnO-FA NPs (b)

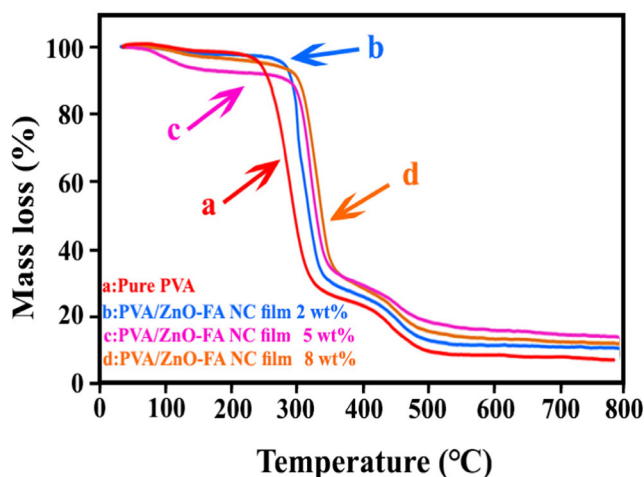


Fig. 14 The TGA curves of the pure PVA (a), and PVA/ZnO-FA NC films of 2 wt% (b), 5 wt% (c), and 8 wt% (d)

was a dramatic increase in T_{max} , which showed a rise of 40 and 50 °C compared with pure PVA, respectively. The spherical structural morphology and the uniform distribution in the polymeric matrix for the ZnO-FA NPs were observed. The mechanical performance of NC films can be improved by optimizing the amounts of NPs. The water CA showed that the polymeric matrix which was occupied with 5 wt% of ZnO-FA NPs has a stronger hydrophobic property than the rest. This feature is because of the firm hydrogen interactions between the agent groups of the modified NPs and polymer, which diminished the number of accessible hydroxyl groups in the NC films and, as a result, decreased the hydrophilicity property. Overall, FA as a modifying agent, and ultrasound irradiation, can be named as useful factors in the non-agglomeration of the NPs. PVA/ZnO-FA NC film 8 wt% showed the good resistance against *E. coli* and *S. aureus* bacteria that this feature is highly regarded in the manufacture of food packaging construction industry, and textile industry, by employing this method known as the green method, other NC films with other properties could be prepared and utilized in the different technologies.

Acknowledgments The authors gratefully acknowledge the Research Affairs Division of Isfahan University of Technology (IUT), Isfahan. I. R. Iran and also, financial support from Iran Nanotechnology Initiative Council (INIC), Tehran, I. R. Iran, National Elite Foundation (NEF), Tehran, I. R. Iran, and Center of Excellence in Sensors and Green

Table 5 The consequences obtained from the thermal stability analysis

Sample	$T_{10\%}$	$T_{50\%}$	CY (%)	T_{max} (°C)
Pure PVA	257	297	7	285
PVA/ZnO-FA NC film 2 wt%	292	319	11	301
PVA/ZnO-FA NC film 5 wt%	286	330	14	325
PVA/ZnO-FA NC film 8 wt%	338	303	12	335

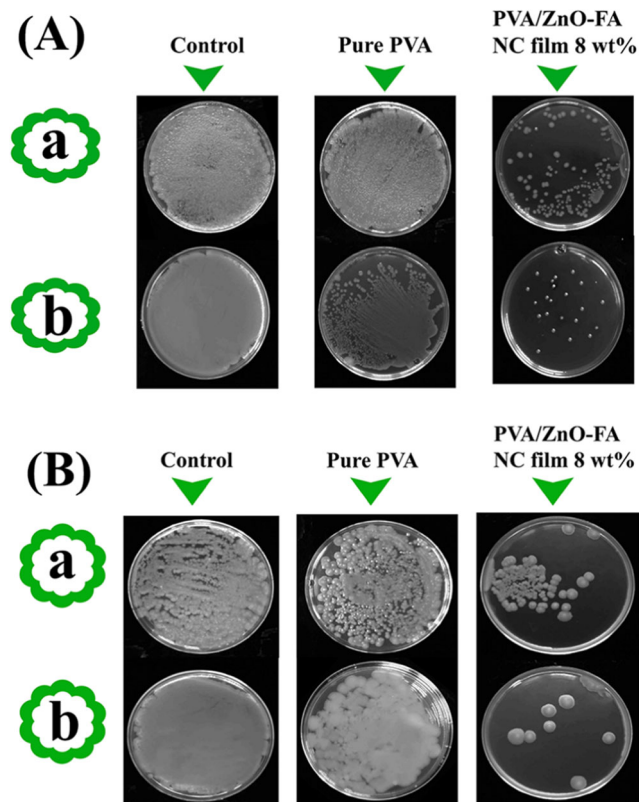


Fig. 15 Antibacterial activity of control sample, pure PVA, and PVA/ZnO-FA NC film 8 wt% against *E. coli* (A) after 24 (a) and 48 h (b), and *S. aureus* (B) after 24 (a) and 48 h (b)

Table 6 The percentages of bacterial inhibition against *E. coli*

Sample / Time	Pure PVA	PVA/ZnO-FA NC film 8 wt%
24 h	0%	48.7%
48 h	0%	72.2%

Chemistry (IUT), Isfahan, I. R. Iran. Also, the authors would like to thank Prof. K. Karami, Dr. V. Behranvand, Miss. E. Azadi, Miss. F. Sirous, Mrs. M. Abbasi, Mrs. B. Seyfi, Miss. F. Sadeghi, Miss. M. Naghdi, Dr. E. Khadem, Dr. F. Azimi, Dr. S. Rashidimoghaddam, Dr. M. Hatami, and Dr. F. Tabesh for the technical assistance and helpful discussions.

Compliance with ethical standards

Conflict of interest The authors declare that they have no conflict of interest.

Table 7 The percentages of bacterial inhibition against *S. aureus*

Sample / Time	Pure PVA	PVA/ZnO-FA NC film 8 wt%
24 h	0%	49.9%
48 h	0%	82.7%

References

- Chiellini E (2008) Environmentally compatible food packaging. Elsevier, London
- Honarvar Z, Hadian Z, Mashayekh M (2016) Nanocomposites in food packaging applications and their risk assessment for health. *Electron Physician* 8:3248–3256
- Liau LC-K, Lin Y-H (2017) Effects of electric fields on the conduction of poly(vinyl alcohol) (PVA)/ZnO films by photoluminescence analysis. *J Lumin* 181:217–222
- Mallakpour S, Khadem E (2016) Recent achievements in the synthesis of biosafe poly(vinyl alcohol) nanocomposite in: Inamuddin (ed) green polymer composites technology. Taylor & Francis Group, Boca Raton, pp 261–278
- Yang X, Guo Y, Han Y, Li Y, Ma T, Chen M, Kong J, Zhu J, Gu J (2019) Significant improvement of thermal conductivities for BNNS/PVA composite films via electrospinning followed by hot-pressing technology. *Compos Part B-eng* 175:107070
- Zhao J, Zhang J, Wang L, Lyu S, Ye W, Xu BB, Qiu H, Chen L, Gu J (2020) Fabrication and investigation on ternary heterogeneous MWCNT@ TiO₂-C fillers and their silicone rubber wave-absorbing composites. *Compos Part A Appl Sci Manuf* 129:105714
- Liang C, Song P, Ma A, Shi X, Gu H, Wang L, Qiu H, Kong J, Gu J (2019) Highly oriented three-dimensional structures of Fe₃O₄ decorated CNTs/reduced graphene oxide foam/epoxy nanocomposites against electromagnetic pollution. *Compos Sci Technol* 181:107683
- SD Praveena I, Ravindrachary V, Bhajantri RF (2014) Dopant-induced microstructural, optical, and electrical properties of TiO₂/PVA composite. *Polym Polym Compos* 16:101–113
- Saini I, Rozra J, Chandak N, Aggarwal S, Sharma PK, Sharma A (2013) Tailoring of electrical, optical and structural properties of PVA by addition of Ag nanoparticles. *Mater Chem Phys* 139:802–810
- Pasha SKK, Deshmukh K, Ahamed MB, Chidambaram K, Mohanapriya MK, Raj NAN (2015) Investigation of microstructure, morphology, mechanical, and dielectric properties of PVA/PbO nanocomposites. *Adv Polym Technol* 36:352–361
- Ghanbari D, Salavati-Niasari M, Ghasemi-Kooch M (2014) A sonochemical method for synthesis of Fe₃O₄ nanoparticles and thermal stable PVA-based magnetic nanocomposite. *J Ind Eng Chem* 20:3970–3974
- Liang C, Song P, Gu H, Ma C, Guo Y, Zhang H, Xu X, Zhang Q, Gu J (2017) Nanopolydopamine coupled fluorescent nanozinc oxide reinforced epoxy nanocomposites. *Compos Part A Appl Sci Manuf* 102:126–136
- Sirohi S, Singh R, Jain N, Pani B, Dutt K, Nain R (2017) Synthesis and characterization of multifunctional ZnO/polyester green composite films. *J Polym Res* 24:193–204
- Fernandes DM, Hechenleitner AAW, Lima SM, Andrade LHC, Caires ARL, Pineda EAG (2011) Preparation, characterization, and photoluminescence study of PVA/ZnO nanocomposite films. *Mater Chem Phys* 128:371–376
- Hemalatha KS, Rukmani K, Suriyamurthy N, Nagabhushana BM (2014) Synthesis, characterization, and optical properties of hybrid PVA-ZnO nanocomposite: a composition dependent study. *Mater Res Bull* 51:438–446
- Gharoy Ahangar E, Abbaspour-Fard MH, Shahtahmassebi NN, Khojastehpour M, Maddahi P (2015) Preparation and characterization of PVA/ZnO nanocomposite. *J Food Process Preserv* 39:1442–1451
- Tang E, Cheng G, Ma X, Pang X, Zhao Q (2006) Surface modification of zinc oxide nanoparticle by PMAA and its dispersion in aqueous system. *Appl Surf Sci* 252:5227–5232

18. Chakradhar RPS, Dinesh Kumar V (2012) Water-repellent coatings prepared by modification of ZnO nanoparticles. *Spectrochim Acta - Part A Mol Biomol Spectrosc* 94:352–356
19. Mallakpour S, Darvishzadeh M (2018) Nanocomposite materials based on poly(vinyl chloride) and bovine serum albumin modified ZnO through ultrasonic irradiation as a green technique: optical, thermal, mechanical and morphological properties. *Ultrason Sonochem* 41:85–99
20. Mallakpour S, Behranvand V (2015) Effect of modified ZnO capped with N-trimellitylimido-L-alanine diacid as an optically active coupling agent on the morphology and thermal properties of poly (amide-imide)/ZnO nanocomposites. *Des Monomers Polym* 18:79–88
21. Mallakpour S, Nouruzi N (2018) Evaluation of ZnO-vitamin B₁ nanoparticles on bioactivity and physicochemical properties of the polycaprolactone-based nanocomposites. *Polym Plast Technol Eng* 57:46–58
22. Mallakpour S, Nouruzi N (2017) Effects of citric acid-functionalized ZnO nanoparticles on the structural, mechanical, thermal and optical properties of polycaprolactone nanocomposite films. *Mater Chem Phys* 197:129–137
23. Abdolmaleki A, Mallakpour S, Borandeh S (2014) Tailored functionalization of ZnO nanoparticle via reactive cyclodextrin and its bionanocomposite synthesis. *Carbohydr Polym* 103:32–37
24. Vora A, Riga A, Dollimore D, Alexander KS (2002) Thermal stability of folic acid. *Thermochim Acta* 392–393:209–220
25. Palanikumar S, Kannammal L, Meenarathi B, Anbarasan R (2014) Effect of folic acid decorated magnetic fluorescent nanoparticles on the sedimentation of starch molecules. *Int Nano Lett* 4:104–113
26. Ma Y-Y, Ding H, Xiong H-M (2015) Folic acid functionalized ZnO quantum dots for targeted cancer cell imaging. *Nanotechnology* 26: 305702
27. Muhammad F, Guo M, Guo Y, Qi W, Qu F, Sun F, Zhao H, Zhu G (2011) Acid degradable ZnO quantum dots as a platform for targeted delivery of an anticancer drug. *J Mater Chem* 21:13406
28. Mallakpour S, Abdolmaleki A, Azimi F (2017) Ultrasonic-assisted biosurface modification of multi-walled carbon nanotubes with thiamine and its influence on the properties of PVC/tm-MWCNTs nanocomposite films. *Ultrason Sonochem* 39:589–596
29. Chen D, Sharma AM SK (2011) *Handbook on applications of ultrasound: sonochemistry for sustainability*. CRC Press, Florida
30. Hadisi Z, Nourmohammadi J, Nassiri SM (2018) The antibacterial and anti-inflammatory investigation of Lawsonia Inermis-gelatin-starch nano-fibrous dressing in burn wound. *Int J Biol Macromol* 107:2008–2019
31. Mohammed MI (2018) Optical properties of ZnO nanoparticles dispersed in PMMA/PVDF blend. *J Mol Struct* 1169:9–17
32. Chung SJ, Leonard JP, Nettleship I, Lee JK, Soong Y, Martello DV, Chyu MK (2009) Characterization of ZnO nanoparticle suspension in water: effectiveness of ultrasonic dispersion. *Powder Technol* 194:75–80
33. Nayunigari MK, Das R, Maity A, Agarwal S, Gupta VK (2017) Folic acid modified cross-linked cationic polymer: synthesis, characterization, and application of the removal of Congo red dye from aqueous medium. *J Mol Liq* 227:87–97
34. Hao J, Tong T, Jin K, Zhuang Q, Han T, Bi Y, Wang J, Wang X (2017) Folic acid-functionalized drug delivery platform of resveratrol based on pluronic 127/D- α -tocopheryl polyethylene glycol 1000 succinate mixed micelles. *Int J Nanomedicine* 12:2279–2292
35. Chen X, Wang Z, Wu J (2019) Processing and characterization of natural rubber/stearic acid-tetra-needle-like zinc oxide whiskers medical antibacterial composites. *J Polym Res* 25:48–60
36. Lai TY, Lee WC (2009) Killing of cancer cell line by photoexcitation of folic acid-modified titanium dioxide nanoparticles. *J Photochem Photobiol A Chem* 204:148–153
37. Mallakpour S, Behranvand V (2014) Optical, mechanical, and thermal behavior of poly(vinyl alcohol) composite films embedded with biosafe and optically active poly(amide-imide)-ZnO quantum dot nanocomposite as a novel reinforcement. *Colloid Polym Sci* 292:2857–2867
38. Mallakpour S, Motirasoul F (2018) Capturing Cd²⁺ ions from wastewater using PVA/ α -MnO₂-oleic acid nanocomposites. *New J Chem* 42:4297–4307
39. Guo J, Liu G, Guo Y, Tian L, Bao X, Zhang X, Yang B, Cui J (2019) Enhanced flame retardancy and smoke suppression of polypropylene by incorporating zinc oxide nanowires. *J Polym Res* 26: 19–30
40. Hafez RS, El-Khiyami S (2020) Effect of copper(II) nitrate 3H₂O on the crystalline, optical and electrical properties of poly (vinyl alcohol) films. *J Polym Res* 27:26–33
41. Siva Vijayakumar T, Karthikeyeni S, Vasanth S, Ganesh A, Bupesh G, Ramesh R, Manimegalai M, Subramanian P (2013) Synthesis of silver-doped zinc oxide nanocomposite by pulse mode ultrasonication and its characterization studies. *J Nanosci* 2013:1–7
42. Mallakpour S, Shafiee E (2018) A simple method for the sonochemical synthesis of PVA/ZrO₂-vitamin B1 nanocomposites: morphology, mechanical, thermal and wettability investigations. *Ultrason Sonochem* 40:881–889
43. Lin CC, Lin YC (2016) Preparation of ZnO nanoparticles using a rotating packed bed. *Ceram Int* 42:17295–17302
44. Liu G, Pang J, Huang Y, Xie Q, Guan G, Jiang Y (2017) Self-assembled nanospheres of folate-decorated zein for the targeted delivery of 10-Hydroxycamptothecin. *Ind Eng Chem Res* 56: 8517–8527
45. Brown GM (1962) The biosynthesis of folic acid. *J Biol Chem* 237: 3299–3302
46. Rithin Kumar NB, Crasta V, Bhajantri RF, Praveen BM (2014) Microstructural and mechanical studies of PVA doped with ZnO and WO₃ composites films. *J Polym* 2014:1–7
47. Mallakpour S, Motirasoul F (2016) Covalent surface modification of α -MnO₂ nanorods with l-valine amino acid by solvothermal strategy, preparation of PVA/ α -MnO₂-l-valine nanocomposite films and study of their morphology, thermal, mechanical, Pb (ii) and cd (ii) adsorption properties. *RSC Adv* 6:62602–62611
48. Sing K (2001) The use of nitrogen adsorption for the characterisation of porous materials. *Colloids Surfaces A Physicochem Eng Asp* 187–188:3–9
49. Reddy CV, Babu B, Shim J (2018) Synthesis, optical properties and efficient photocatalytic activity of CdO/ZnO hybrid nanocomposite. *J Phys Chem Solids* 112:20–28
50. Mallakpour S, Hatami M (2017) Biosafe organic diacid intercalated LDH/PVC nanocomposites versus pure LDH and organic diacid intercalated LDH: synthesis, characterization, and removal behaviour of Cd²⁺ from aqueous test solution. *Appl Clay Sci* 149:28–40
51. Mallakpour S, Yazdan Nazari H (2018) The influence of bovine serum albumin-modified silica on the physicochemical properties of poly(vinyl alcohol) nanocomposites synthesized by ultrasonication technique. *Ultrason Sonochem* 41:1–10
52. Zhao T, Jiang L (2018) Contact angle measurement of natural materials. *Colloids Surfaces B Biointerfaces* 161:324–330
53. Mallakpour S, Behranvand V (2017) Sono-assisted preparation of bio-nanocomposite for removal of Pb²⁺ ions: study of morphology, thermal, and wettability properties. *Ultrason Sonochem* 39:872–882
54. Mallakpour S, Javadpour M (2017) Host recycled poly(ethylene terephthalate) and guest PVA-grafted ZnO nanoparticles: prepared nanocomposites characterization. *Polym Bull* 75:1–16
55. Xiao R, Wang W, Pan L, Zhu R, Yu Y, Li H, Liu H, Wang SL (2011) A sustained folic acid release system based on ternary magnesium/zinc/aluminum layered double hydroxides. *J Mater Sci* 46: 2635–2643

56. Ahad N, Saion E, Gharibshahi E (2012) Structural, thermal, and electrical properties of PVA-sodium salicylate solid composite polymer electrolyte. *J Nanomater* 2012:94–102
57. Rasad MSBA, Kumar A, Yusoff MM, Chahal S, Hussain FSJ (2016) Fabrication, characterization and in vitro biocompatibility of electrospun hydroxyethyl cellulose/poly(vinyl alcohol) nanofibrous composite biomaterial for bone tissue engineering. *Chem Eng Sci* 144: 17–29r
58. Yang X, Li L, Shang S, Ming TX (2010) Synthesis and characterization of layer-aligned poly(vinyl alcohol)/graphene nanocomposites. *Polymer* 51:3431–3435
59. Mersian H, Alizadeh M, Hadi N (2018) Synthesis of zirconium doped copper oxide (CuO) nanoparticles by the Pechini route and investigation of their structural and antibacterial properties. *Ceram Int* 44:20399–20408
60. Mallakpour S, Mansourzadeh S (2018) Sonochemical synthesis of PVA/PVP blend nanocomposite containing modified CuO nanoparticles with vitamin B1 and their antibacterial activity against *Staphylococcus aureus* and *Escherichia coli*. *Ultrason Sonochem* 43:91–100
61. Espitia PJP, de FF SN, dos Reis CJS, de Andrade CNJ, Cruz RS, EAA M (2012) Zinc oxide nanoparticles: synthesis, antimicrobial activity, and food packaging applications. *Food Bioprocess Technol* 5:1447–1464

Publisher's note Springer Nature remains neutral with regard to jurisdictional claims in published maps and institutional affiliations.